PERGAMON

Carbon 39 (2001) 2065–2075

CARBON

Microstructure and mechanical properties of coal tar pitch-based 2D-C/C composites with a filler addition

G. Chollon[a,*], O. Siron[a], J. Takahashi[a], H. Yamauchi[b], K. Maeda[b], K. Kosaka[b]

[a]*National Institute of Materials and Chemical Research, Department of Composite Materials, 1-1 Higashi, Tsukuba, Ibaraki 305-8565, Japan*

[b]*Nissan Motor Co. Ltd., Tomioka Plant, Aerospace Division 900, Fujiki, Tomioka, Gunma 370-2398, Japan*

Received 6 November 2000; accepted 22 January 2001

Abstract

In order to improve the flexural and the inter-laminar shear strength of coal tar pitch-based 2D-C/C composites, fillers (carbon blacks and colloidal graphite) have been introduced between the UD layers before the first infiltration of pitch. Matrix parts made of the filler/pitch-based cokes showed fine mosaic microtextures. They were found at the interface between the layers. Whereas the tensile strength is not affected, the flexural strength and the ILSS were significantly increased by the addition of fillers. The original structure of the inter-layer matrix parts and the decrease of the number of flaws were found to be responsible for the improvement of the shear strength of the 0/90° UD layers.

Keywords: A. Carbon/carbon composites, Coal tar pitch; C. Raman spectroscopy; D. Microstructure, Mechanical properties

1. Introduction

Coal tar pitches are excellent carbon matrix precursors for the manufacturing of carbon/carbon (C/C) composites because of their low price, high density and high carbon yield. However, because of their plasticity and devolatilisation during the early stage of carbonisation [1] and the further shrinkage of the cokes during pyrolysis, many pores and cracks are observed in the composite after the first infiltration/carbonisation cycle. Further cycles are therefore necessary to achieve proper density and mechanical properties [2]. The initial void structure resulting from the processing of the coal tar pitch-based 2D-C/C composites significantly affects their mechanical properties [2–6]. For instance, coplanar inter-layer flaws due to processing are obviously expected to affect the inter-laminar shear strength (ILSS) (a critical property of 2D-C/C composites), as it is for phenolic resin-based composites [7].

It has been shown that the addition of carbon blacks increases the carbon yield, the strength and decreases the porosity and the crystal size of the pitch-based cokes [8,9]. The aim of this study is to report the influence of the addition of carbon blacks and colloidal graphite to the coal tar pitch precursor, on the mechanical properties of the 2D-C/C composites. The fillers have been more especially introduced between the layers in order to improve the inter-layer bonding and ILSS.

2. Experimental

2.1. Materials

The 2D-C/C composites were prepared from unidirectional plies of high modulus Carbonic HM80 fibres from Petoca Ltd. [10]. Suspensions of carbon blacks (CB) (no. 40 from Mitsubishi Kasei Co. Ltd., Tokyo, Japan, with an average size equal to 24 nm and a specific surface equal to 125 $m^2\ g^{-1}$) and colloidal graphite (CG) (GP-60 from Hitachi Funmatsu Yakin Kugyu, Tokyo, Japan, with particle sizes ranging from 1 to 6 μm) were spread on the surface of the plies. The UD prepregs were stacked according to a 0/90° sequence of 14 plies. The thickness was controlled to reach a volume fraction of fibres equal to

*Corresponding author. Present address: Laboratoire des Composites Thermostructuraux, 3, Allée de La Boétie, Université de Bordeaux 1, F-33600 Pessac, France. Fax: +33-5-56-84-12-25.

E-mail address: chollon@lcts.u-bordeaux.fr (G. Chollon).

0008-6223/01/$ – see front matter
PII: S0008-6223(01)00021-5

60% and the amount of filler was adjusted to a weight ratio of matrix ranging from 0 to 20%. The preform was successively infiltrated with coal tar pitch, carbonised by hot isostatic pressing (HIP) at 650°C and graphitised at 2400°C. This procedure was repeated three times to achieve a proper densification.

2.2. Microstructural characterisation

The polished cross sections of the 2D-C/C composites were examined with polarized light microscopy to analyse the fibrous structure and the voids of the composite and the optical texture of the pitch-based matrix.

The samples were also submitted to Raman microspectroscopy (RMS). The Raman microspectrometer used was a Renishaw 2000 (Renishaw plc., Wollon-under-Edge, UK) and the monochromatic light exciting source was the 514.5 nm line of an Ar^+ laser. The laser beam was focused on the samples with a 50× objective onto a spot 1–2 μm in diameter. Its power was less than 1.5 mW to avoid heating the sample and a shift of the Raman peaks. The spectrometer and the detector system is described elsewhere [11]. The grating was set at a constant tilt angle during the measurements, the CCD detector providing a spectral range of about 1000–1800 cm^{-1}. The spectra were calibrated with the frequency of diamond (ν=1332.0 cm^{-1}). The two main peaks investigated correspond to the first order E_{2_g} vibrational mode of graphite at about 1580 cm^{-1} and the mode associated to disordered carbon at about 1350 cm^{-1}. Their characteristics (frequency ν, width at half height $\Delta\nu$, intensity I) were determined by fitting the data to a Lorentzian shape.

The density of the materials was assessed from geometrical measurements (geometrical density) and from weight measurements in air and water after evacuation to take the open porosity into account (apparent density).

2.3. Mechanical characterisation

The tensile, flexural and inter-laminar shear strengths were measured using a universal testing machine. The 200×20 mm dog bone specimens (with a 75 mm gauge length) were tensile tested with a cross head speed (CHS) equal to 1 mm/min). The longitudinal strain was measured using two strain gages mounted on both opposite sides of the specimens. Flexural tests were performed according to the four-point bending method using 100×10 mm specimens loaded at 1 mm/min in CHS, between two support rollers with span equal to 27 and 81 mm, respectively. The strain of the tensile-tested side of the specimens was measured with a strain gage. The ILSS was measured from compact three-point bending tests. The 14×10 mm specimens were loaded at a CHS equal to 1 mm/min between a 6 mm roller and a two 4 mm support rollers, 10 mm apart. Five different specimens were tested for each testing procedure and each filler ratio.

3. Results and discussion

In the various 2D-C/C composites, voids can be classified into different groups. Devolatilisation pores are located within or between the unidirectional (UD) fibre layers (Figs. 1 and 2). They are homogeneously distributed but seldom observed whatever the nature and the amount of filler. Their size is generally small (around 10 μm) owing to the HIP carbonisation process. Large (several tenths of microns) intra-layer cracks parallel to the fibre axis and running through the thickness of the UD layers are also observed. Their number along the length of the layers is also approximately independent of the nature and the amount of filler. These cracks can be attributed to the shrinkage of the pitch-based coke infiltrated within the fibre bundle. They appear during the first infiltration/carbonisation/graphitisation cycle and are only partially filled during further impregnation cycles. Additionally, large coplanar inter-layer cracks are observed in the composites. They generally run straight between the 0 and 90° layers in the composites with a low filler addition and their number and length significantly decrease with the amount of filler. A delamination of the composite with a 3 wt.% ratio of CG was sometimes observed during the machining of the samples, probably owing to faulty processing conditions resulting in a high number of such flaws. Inter-layer cracks likely originate from the mismatch between the favoured directions of shrinkage of two successive 0 and 90° layers. They might also appear during processing at high-temperature, owing to the coefficient of thermal expansion mismatch between the 0 and 90° layers [10].

The various pitch-based cokes resulting from the addition of fillers are easily discernible. The pure pitch-based coke forms large anisotropic domains of graphite-like carbon (several tenths of microns). It is always found within the fibre bundles and between the layers of the composites with a low filler addition (Fig. 2). The filler/pitch-based matrix parts are only found between the layers or infiltrates only superficially the fibre bundles for the highest filler ratios (Figs. 3–5). Their fraction regularly increases with the filler ratio, from small and isolated domains for a 3 wt.% ratio (Fig. 3), to thick sub-layers almost free of fibres for a 20 wt.% ratio (Figs. 4 and 5), suggesting that fillers diffuse only very locally within the fibre bundle during the processing. The CB/pitch-based matrix parts exhibited a fine sub-micrometric microstructure and were found to be isotropic by polarized light microscopy (Figs. 3 and 4). Conversely, the CG/pitch-based coke shows a coarser mosaic texture with domains homogenous in size, up to several microns (Fig. 5).

The fibres and the matrix were investigated from polished sections, perpendicular to the fibre axis. The Raman spectrum of the first order region (1000–1800 cm^{-1}) of the materials tested generally showed two main prominent peaks at 1581–1585 cm^{-1} and 1352–1355

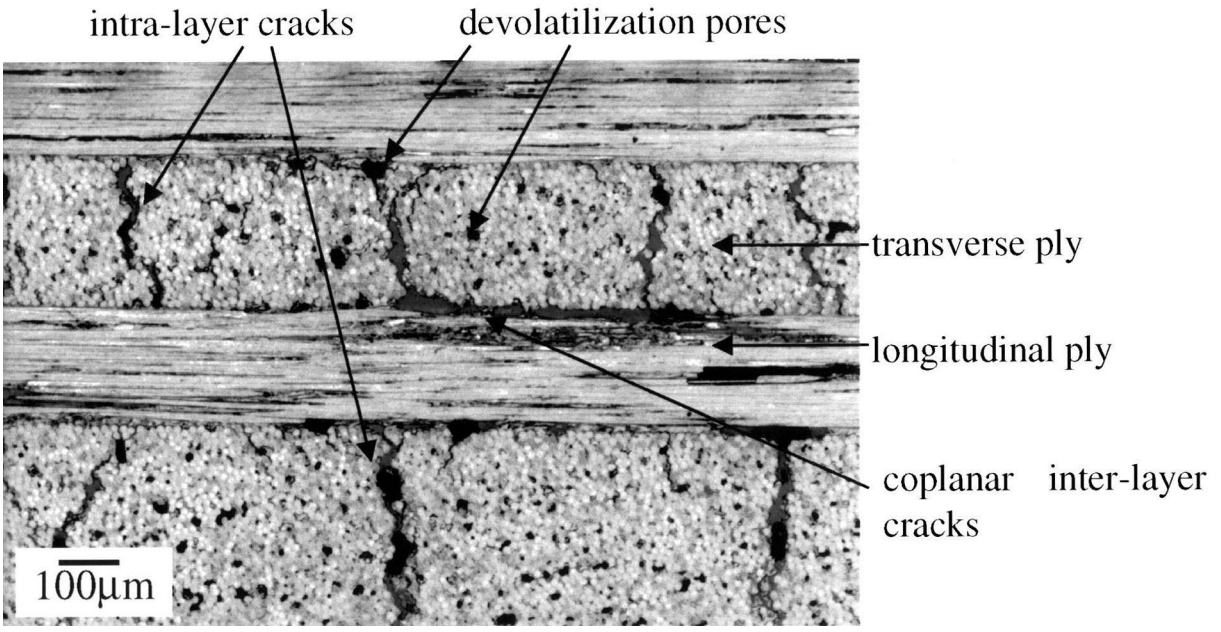

Fig. 1. Optical micrograph of the 2D-C/C composite without filler addition (white light).

cm^{-1} and an additional weak peak at about 1620 cm^{-1} (Fig. 6). These features correspond to the typical vibration modes encountered in low ordered carbon materials (e.g., turbostratic carbon) and graphite. The first peak (G), with the E_{2_g} symmetry, is assigned to the vibrational mode of graphite single crystal (in-plane C–C stretching within the graphene sheets). The two other peaks at 1352–1355 cm^{-1} (D) and about 1620 cm^{-1} (D′) are observed together with a broadened G peak in polycrystalline or unorganised carbon [12–14]. The enhancement of the crystallinity of

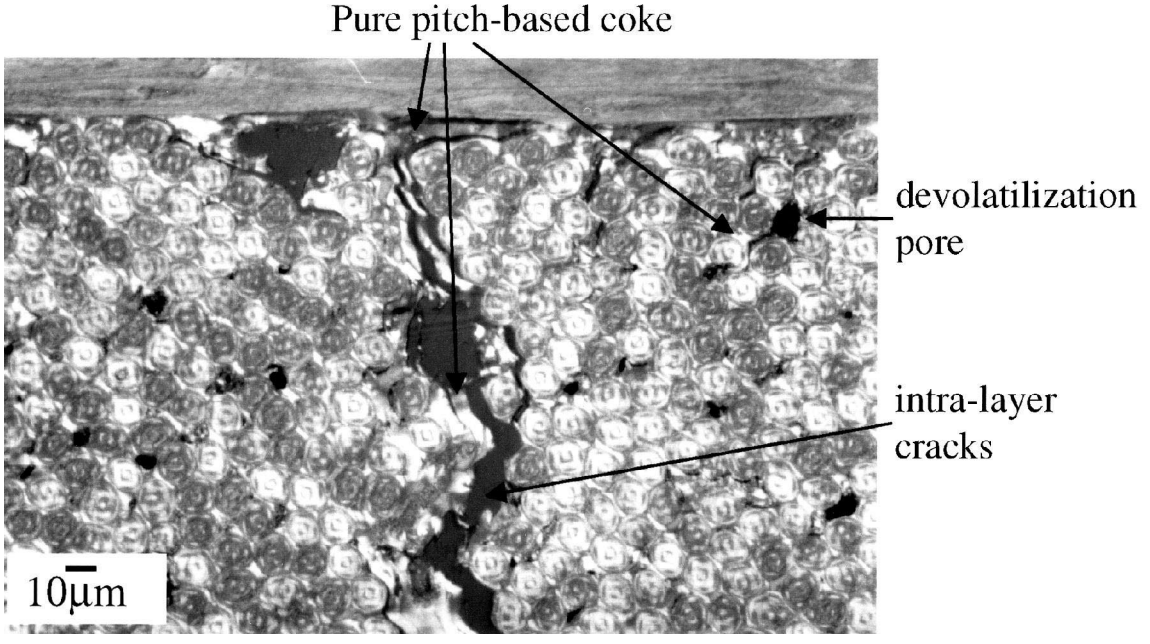

Fig. 2. Optical micrograph of the 2D-C/C composite without filler addition (polarized light).

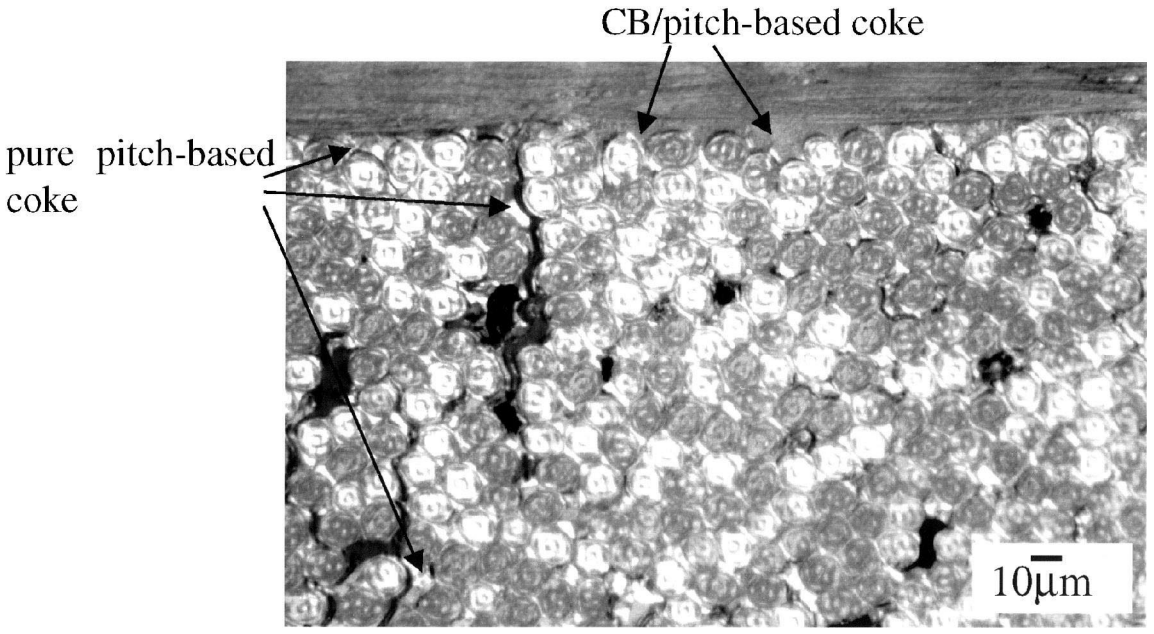

Fig. 3. Optical micrograph of the 2D-C/C composite with a 3 wt.% carbon black (CB) ratio (polarized light).

carbon materials (which is activated for instance by high-temperature or high-pressure) generally results in (i) a decrease of ν_G to the value for graphite (here 1581.0 cm^{-1} for highly orientated pyrolytic graphite, HOPG), (ii) a decrease of $\Delta\nu_G$ and (iii) a decrease of the I_D/I_G ratio [15,16]. These features are directly related to the two dimensional ordering of the carbon domains or crystallites, e.g., the increase of the size of the carbon domains, L_a [12]. Moreover, for highly textured materials, whereas both ν_G and $\Delta\nu_G$ values remain almost unchanged, the I_D/I_G ratio strongly depends on the orientation the carbon basal planes with respect to the incident laser beam.

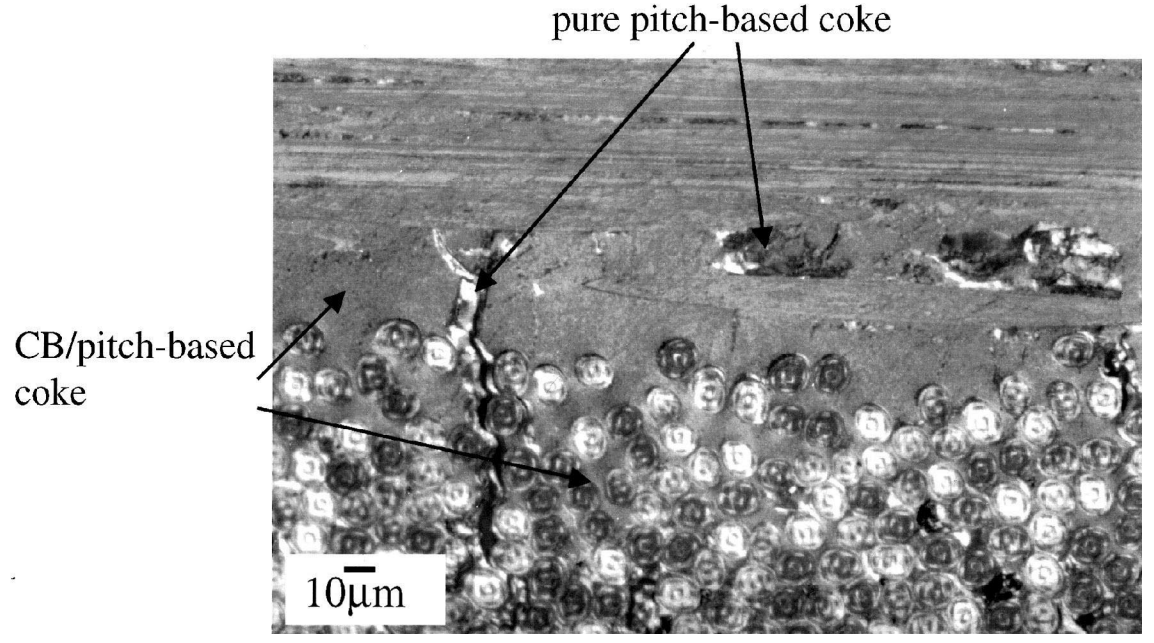

Fig. 4. Optical micrograph of the 2D-C/C composite with a 20 wt.% CB ratio (polarized light).

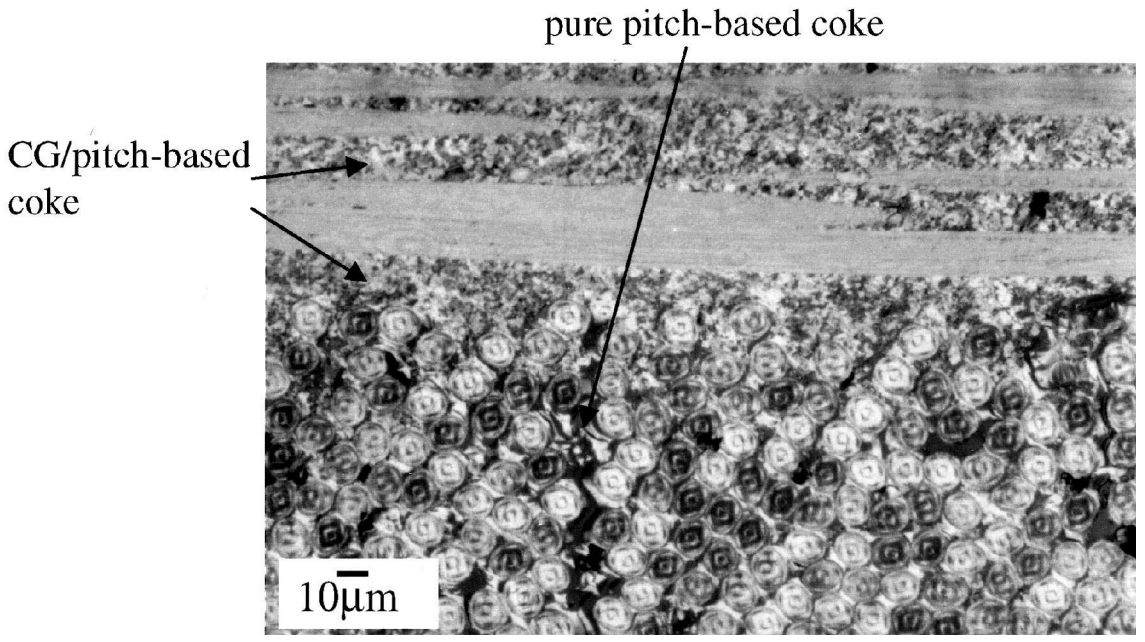

Fig. 5. Optical micrograph of the 2D-C/C composite with a 20 wt.% CG ratio (polarized light).

Hence, for a cross-section of a tilted HOPG crystal, I_D/I_G is directly related to the amount of basal plane edges exposed to the laser beam [17]. Similarly to other carbon materials, the Raman spectral parameters obtained for all the materials tested in the present study follow common relationships. The first one shows a remarkable linear correlation between ν_G and $\Delta\nu_G$, both level decreasing with improving crystalline state, whereas the second one associating ν_G and I_D/I_G, is more complex but still explicit, both parameters decreasing again with improving crystalline state (Fig. 7). Hence, a simple examination of the Raman spectral parameters clearly confirms the higher crystallinity of both the pure pitch and CG/pitch-based cokes, with respect to the CB/pitch-based coke (as already suggested by polarised microscopy). Furthermore, it is worthy of note that, though relatively close in average, the distribution of ν_G, $\Delta\nu_G$ but more especially I_D/I_G is significantly broader for the pure pitch-based coke than for the CG/pitch-based coke. This feature is consistent with the high homogeneity in size and the isotropic texture of the latter material, compared to the highly anisotropic and elongated carbon domains of the former, as already suspected by the optical microscopy observations.

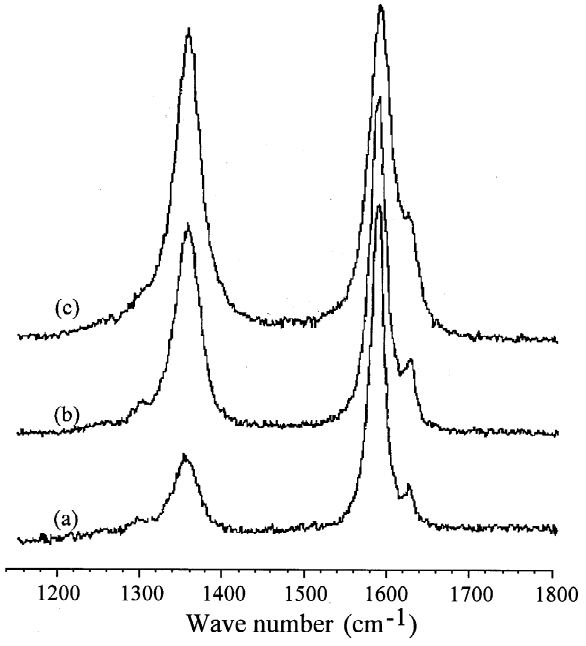

Fig. 6. Raman spectra of pure pitch-based matrix (a), CG/pitch-based matrix (b) and CB/pitch-based matrix (c).

The evolution of both the geometrical density and the apparent density (taking the open porosity into account) of the composites is shown in Fig. 8. The apparent density is remarkably high (up to 2.1 gcm^{-3}). Such a high value is related to the high density of the graphite-like pitch-based coke, the high density of the fibres (2.2 gcm^{-3}), their high volume fraction and the low amount of closed porosity related to the cycling HIP/carbonisation/graphitisation process. However, it slightly decreases with the amount of filler, suggesting that the filler/pitch-based cokes, with their finer texture, have a lower density than the pure pitch-based matrix (while the closed porosity, associated to the pure pitch-based coke and mainly located within the

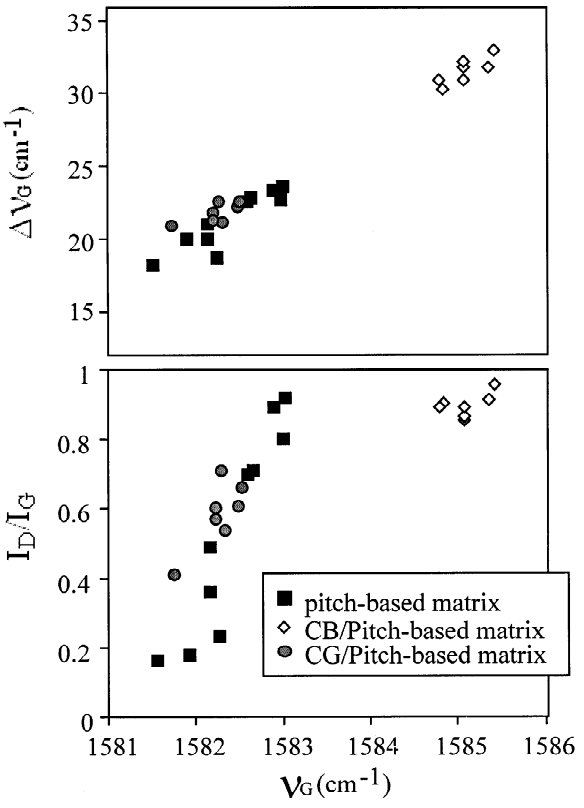

Fig. 7. Raman features of the different matrix parts of the 2D-C/C composites.

fibre bundles, remains almost constant in all composites). The geometrical density exhibits almost the same behaviour as the apparent density, with a slight decrease with the filler ratio, except for the composites with an addition of 3 wt.% of CG and 20 wt.% of CB. Accordingly, the open porosity calculated from the density measurements currently ranges from 4.3 to 5.8% for all composites, except for the composites with an addition of 3 wt.% of CG and 20 wt.% of CB, which have higher values, close to 7%. The low geometrical density of the former might originate from the large macroscopic inter-layer flaws evidenced by optical microscopy and which were assumed to be responsible for the delamination of the composite during machining.

The stress–strain tensile behaviour of the various composites tested is linear up to the brittle failure of the samples. No inelastic strain was observed. The tensile failure strength (σ^R) of the composites is plotted versus the amount of filler in Fig. 9. It typically ranges from 300 to 600 MPa and is not significantly influenced by the filler ratio. A simple rule of mixture calculation, as well as a strain to failure value close to that of the UD composite [18], demonstrates that the Young's modulus and the

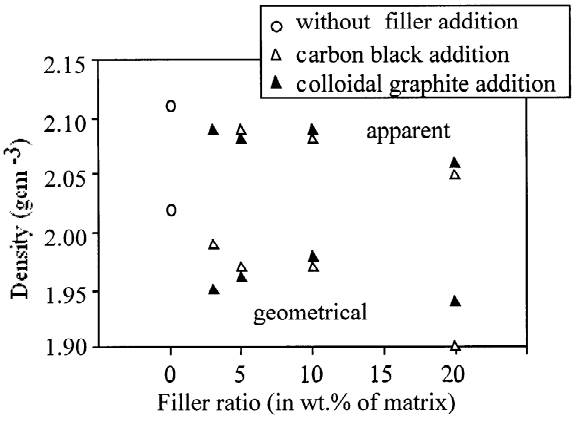

Fig. 8. Density of the 2D-C/C composites.

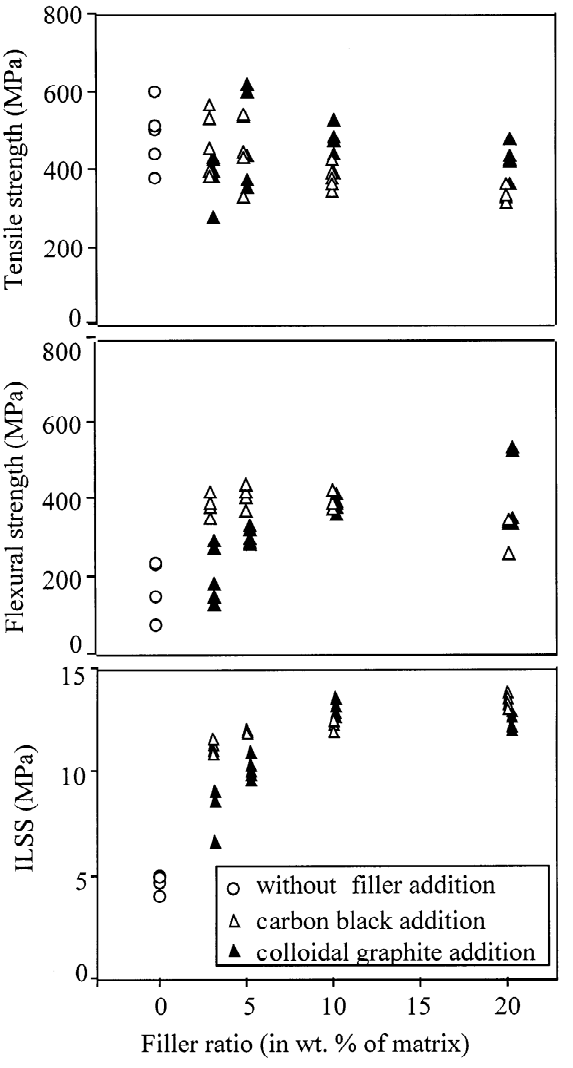

Fig. 9. Mechanical properties of the 2D-C/C composites.

failure of the 2D-C/C composites is essentially controlled by the behaviour of the UD longitudinal plies and more especially by the high modulus and the high strength fibres ($E = 790$GPa and $\sigma^R = 3500$ MPa) [10]. The early damaging observed in the composite under loading that might be initiated from the transverse intra-layer and inter-layer cracks (possibly interconnected) has no apparent effect on the stiffness and the strain to failure of the composite [18]. The fracture is rather induced by the propagation of longitudinal intra-layer cracks and/or the fracture of the fibres and is therefore only little influenced by the filler/pitch-based matrix parts located between the UD layers.

The flexural strength of the composites is presented versus the filler ratio in Fig. 9. A first increase in flexural strength is observed from a filler ratio of 0 to 3 wt.%. It is followed, for higher filler ratios, by a slight further increase from 200 MPa and a plateau up to almost 400 MPa. The exceptional low properties of the composite with a 3 wt.% ratio of CG can be explained by the presence of large macroscopic inter-layer flaws (likely due to faulty processing) which are responsible for the delamination of the composite. The stress–strain relationship is mainly linear for all composites until the maximum loading point. In the case of the composites without filler addition, the failure of the specimens mainly occurred through a delamination process. Fig. 10 shows a typical low magnification view of a specimen where the fracture occurred, in the central part of the composite, between two successive 0/90° plies. In this case, the fracture obviously developed straight through the processing inter-laminar voids between the 0/90° plies, without any deviation within the UD plies, nor any further damaging of the specimen. For the composites with a high filler ratio, the failure generally occurred between the loading noses, on the compressive-tested side of the specimens. As an example, a typical view of a fractured specimen with a 20 wt.% ratio of CG is

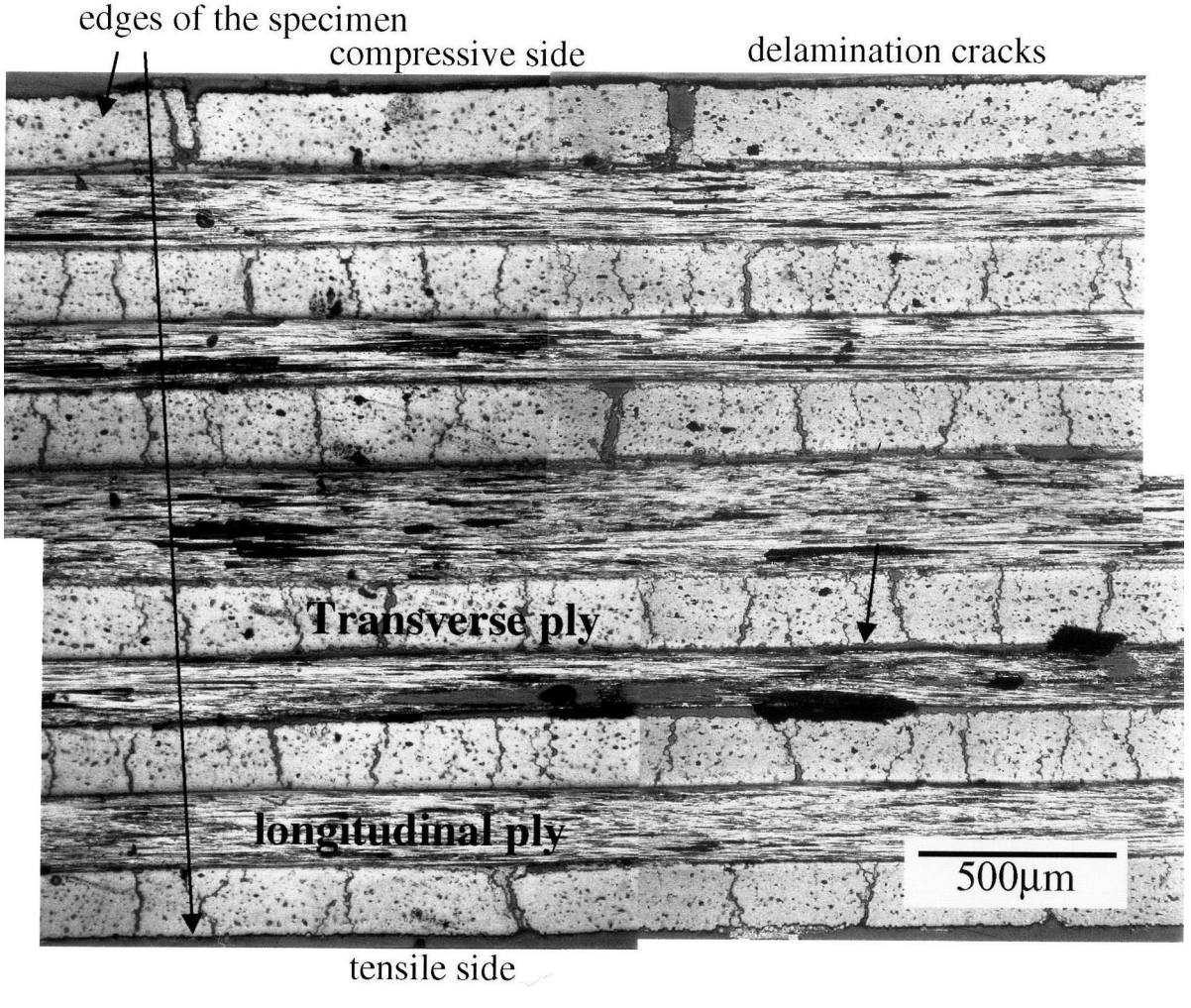

Fig. 10. Optical micrograph showing the fracture process in a 2D-C/C composite without filler addition, under a four point-bend test.

shown in Fig. 11. The fracture process involves, in that case, located shear bands within the longitudinal plies, interspersed with intra and inter-layer delamination cracks [18]. The processing cracks and flaws within the filler/pitch-based coke interlaminar interphase initiate a favoured path for the inter-laminar crack propagation.

The ILSS exhibits a behaviour very similar to that of the flexural strength, with a first significant increase observed for a 3 wt.% filler addition, followed by a slight further increase up to 13 MPa for higher filler ratios. Similarly to the flexural strength, the low ILSS of the composite with a 3 wt.% ratio of CG is assigned to the presence of large processing inter-layer flaws. The fracture mechanisms involved in both the flexural and the inter-laminar shear tests are likely similar. Both the flexural strength and the ILSS are thought to be significantly controlled by the bonding and the shear strength of two successive 0 and 90° UD layers. For all composites, the inter-laminar processing flaws favour the initiation and the propagation of the inter-laminar cracks which are responsible for the delamination of the composite. The flexural and the inter-laminar shear strength obviously both tightly depend on the number of inter-layer cracks existing in the material in the initial state, their orientation and their ability to propagate under loading. Composites with a low filler ratio are characterised by a large number of flat inter-layer cracks. Furthermore, the UD layers are bonded through highly anisotropic pure pitch-based coke, with a basal orientation parallel to the layer, which leads to a particularly low shear resistance. Composites with such microstructure are therefore expected to have a low flexural strength and ILSS. The composites with a higher filler ratio show significantly less coplanar inter-layer cracks. However, some transverse intra-layer cracks, due to shrinkage at high-temperature are still observed. These cracks run through the filler/pitch-based matrix at the interface between the layers. The filler-based cokes are characterised by a finer isotropic texture (especially for the CB-based coke). This type of matrix is expected to be significantly harder and more shear resistant than the pure pitch-based matrix. As a matter of fact, the addition of carbon blacks to coal tar and petroleum pitches was reported to lead to cokes with significantly improved crushing strength [9]. The filler-based coke acts as an effective inter-layer crack deflector

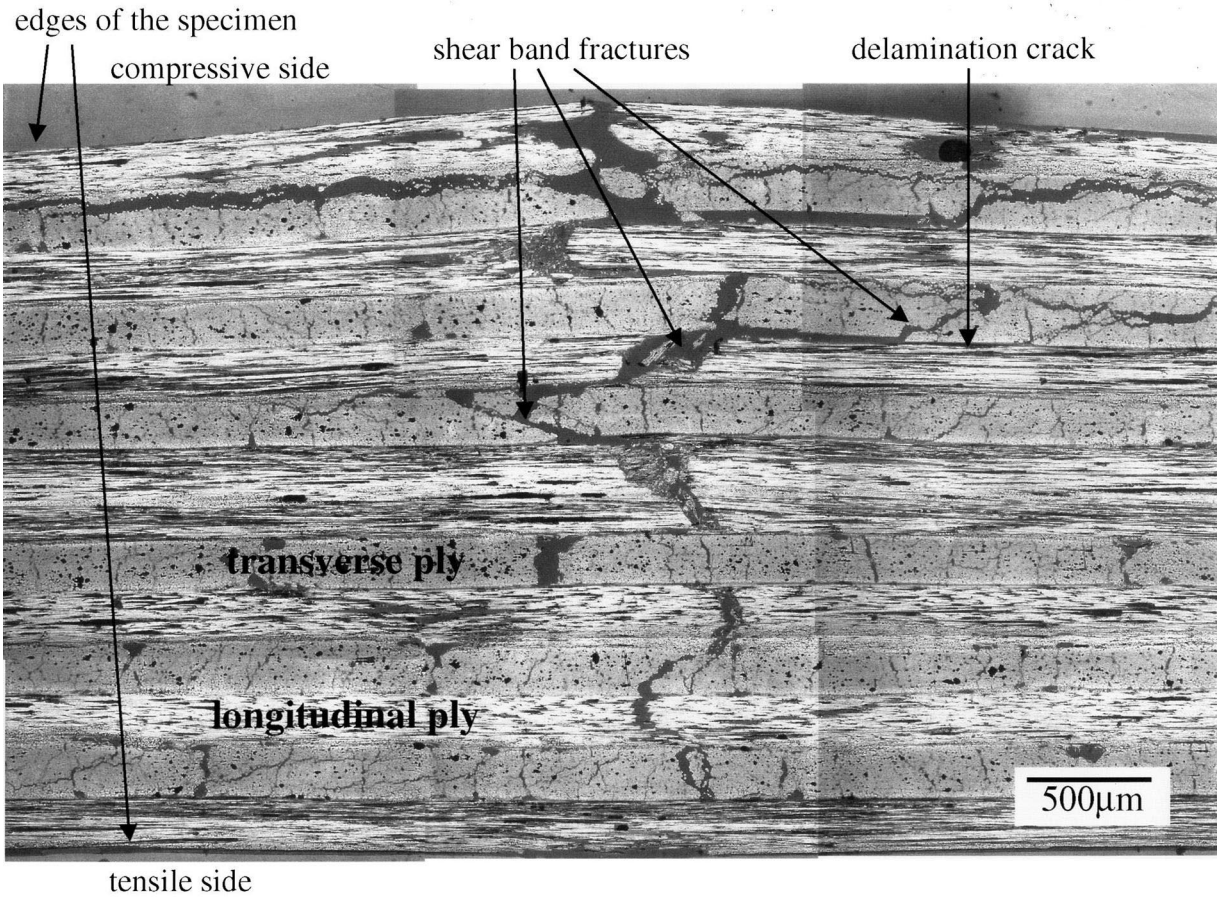

Fig. 11. Optical micrograph showing the fracture process in a 2D-C/C composite with a 20 wt.% CG ratio, under a four point-bend test.

in the case of low filler ratios. Hence, more tortuous inter-laminar cracks (with lower propagation tendency) result and lead to a higher inter-laminar shear resistance of the composites. The effect of the filler is even more beneficial for higher filler ratios. SEM micrographs of the fractured surfaces of composites without and with 20% of GC and submitted to inter-laminar shear tests are shown in Figs. 12 and 13, respectively. The filler-free material shows a flat surface with a low roughness of the order of the radius of the fibres (Fig. 12a). At higher magnification, the material evidences the smooth anisotropic pure pitch-based matrix bridging the 0/90° UD plies, as well as the

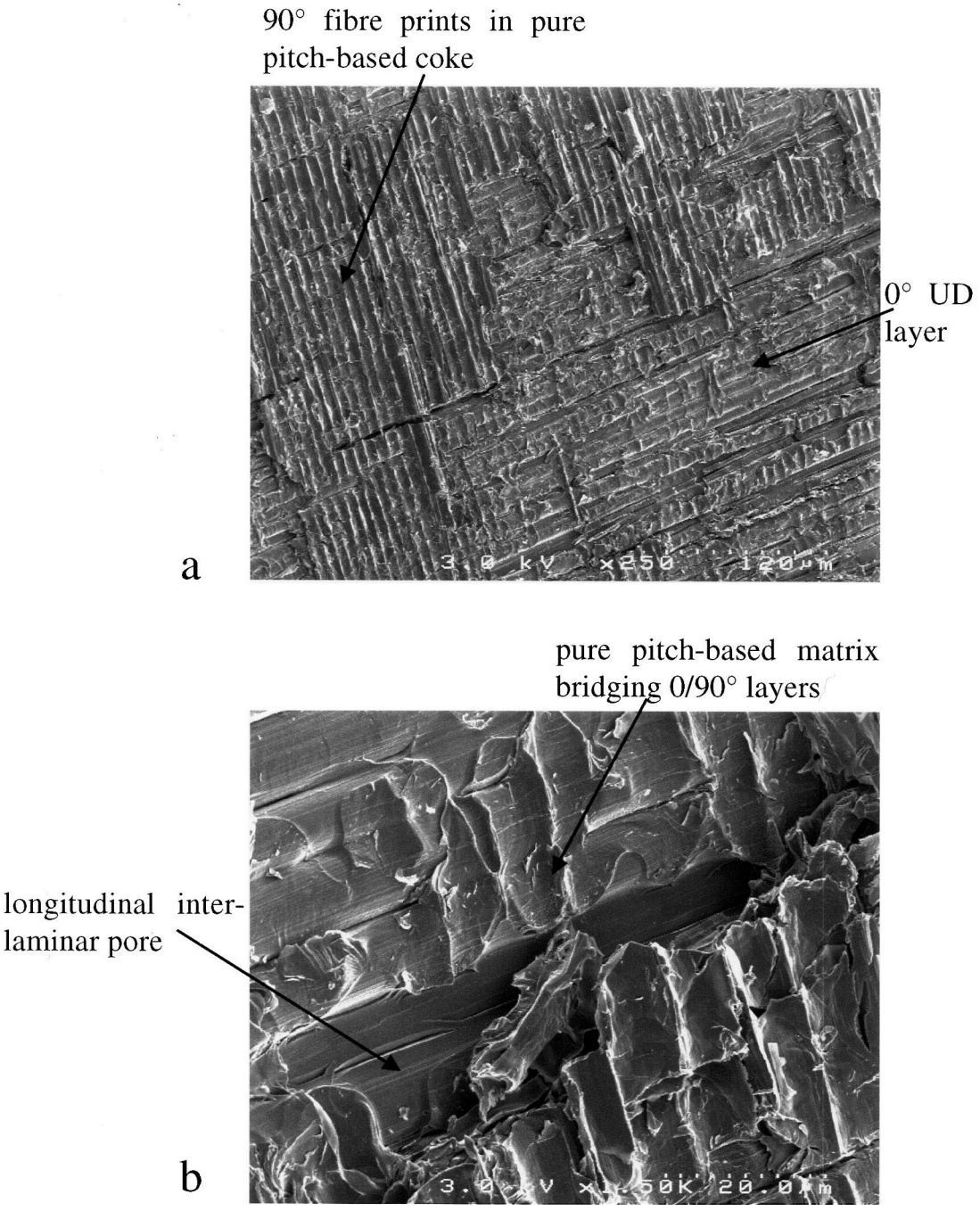

Fig. 12. SEM micrograph showing the fracture surface of a 2D-C/C composite without filler addition, under ILS test.

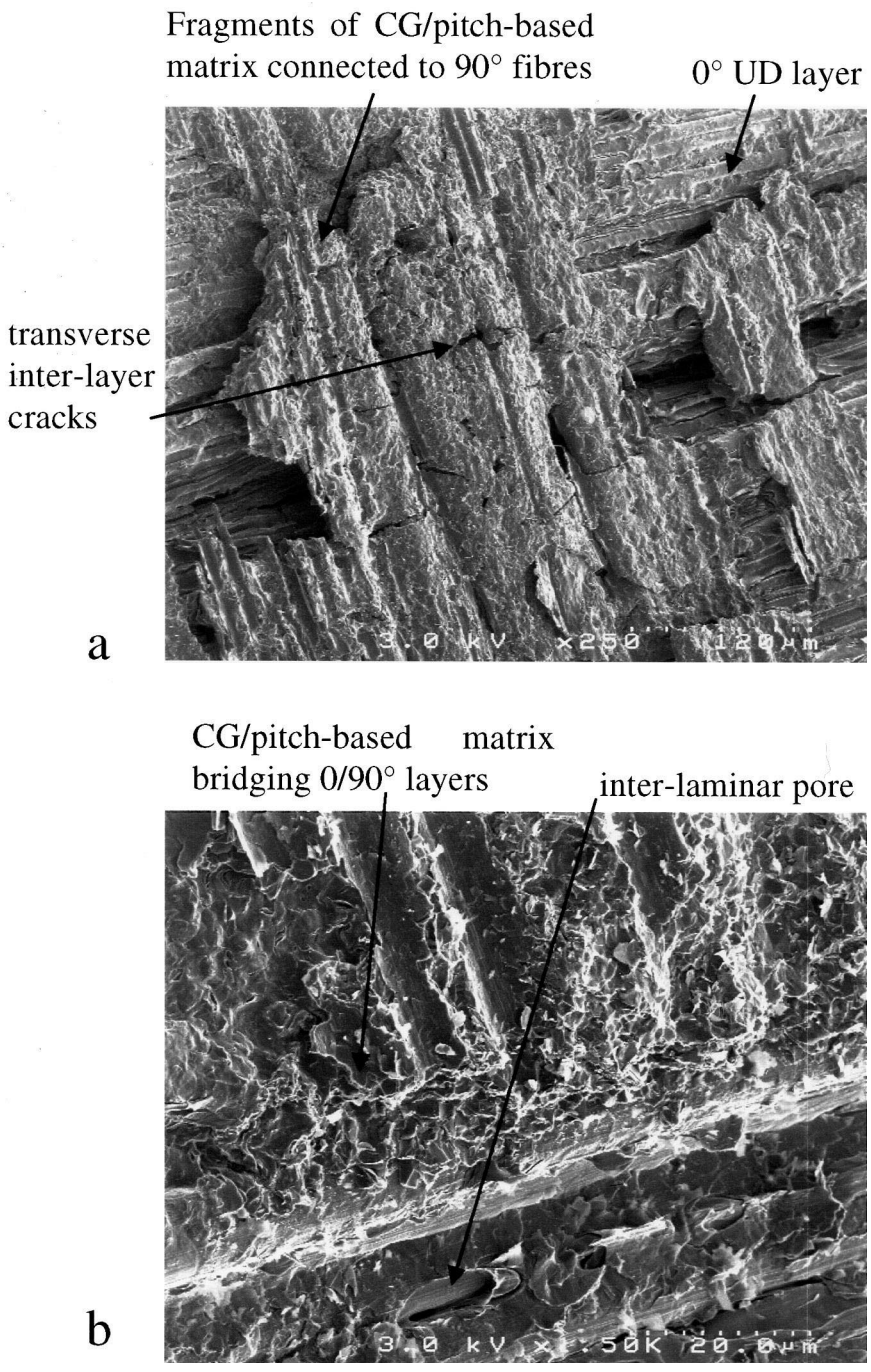

Fig. 13. SEM micrograph showing the fracture surface of a 2D-C/C composite with a 20 wt.% CG ratio, under ILS test.

interlayer pores, responsible for the particularly weak ILSS (Fig. 12b). Conversely, the fracture surface of the composite with a high CG ratio shows a rough surface, large flaws (tenths to hundreds of micrometers), some pullout of large filler-based matrix fragments and fibre failures (Fig. 13a). The dense and rough microstructure of the CG/pitch-based matrix bridging two successive 0/90° plies is clearly evidenced by the high magnification view of the composites (Fig. 13b). Hence, it clearly appears that for higher filler ratios, the partial infiltration of the filler-based matrix within the fibre bundles, forming a high toughness anchoring sub-layer, even further reinforces the bonding between

the 0 and 90° layers and therefore increases both the flexural strength and the ILSS.

4. Conclusion

Various ratios of carbon blacks or colloidal graphite have been introduced between the 0/90° UD layers of a 2D fibrous preform before the first infiltration of coal tar pitch. The addition of filler gives rise to matrix parts with specific microstructures located between the UD layers. The pure pitch-based coke gives rise to large and highly anisotropic domains. The CB/pitch-based coke is isotropic with a fine sub-micrometric texture whereas the CG/pitch-based coke shows a coarser mosaic texture. The volume fraction of these original cokes increases with the filler ratio, from isolated domains to thick sub-layers. While the tensile strength is little influenced by the increase of the filler ratio, the flexural strength and the ILSS both significantly increase. (i) The decrease of the number of inter-layer flaws resulting from the filler addition, (ii) the original microtexture of the filler/pitch-based cokes, which are expected to be more shear resistant than the pure pitch-based coke and (iii) the particular inter-layer arrangement of these though filler-based matrix parts, anchoring the successive UD-layers, are responsible for the improvement of the shear strength of the 0/90° UD layers and therefore the flexural strength and ILSS.

Acknowledgements

This work was supported by the Japanese Ministry of International Trade and Industry through Science and Technology Agency granting. The authors gratefully thank H. Shimura from the Mechanical Engineering Laboratory in Tsukuba, for his assistance with the Raman analyses.

References

[1] Kanno K, Fernandez JJ, Fortin F, Korai Y, Mochida I. Modifications to carbonization of mesophase pitch by addition of carbon blacks. Carbon 1997;35:1627–37.
[2] Granda M, Patrick JW, Walker A, Casal E, Bermejo J, Menendez R. Densification of unidirectional C/C composites by melted pitch impregnation. Carbon 1998;36:943–52.
[3] Gao F, Patrick JW, Walker A. The characterization of cracks and voids in two dimensional carbon–carbon composites. Carbon 1993;31:103–8.
[4] Matzinos PD, Patrick JW, Walker A. Coal-tar pitch as a matrix precursor for 2D-C/C composites. Carbon 1996;34:639–44.
[5] Matzinos PD, Patrick JW, Walker A. The void structure of 2D-C/C preforms and composites: effect of the nature of the matrix precursor coal-tar pitch. Carbon 1997;35:507–13.
[6] Matzinos PD, Patrick JW, Walker A. The efficiency and mechanism of densification of 2D-C/C composites by coal-tar pitch impregnation. Carbon 2000;38:1123–8.
[7] Anand K, Gupta V. The effect of processing conditions on the compressive and shear strength of 2D carbon–carbon laminates. Carbon 1995;33:739–48.
[8] Menendez R, Fernandez JJ, Bermejo J, Cebolla V, Mochida I, Korai Y. The role of carbon black/coal-tar pitch interactions in the early stage of carbonization. Carbon 1996;34:895–902.
[9] Aggarwal RK, Bhatia G. Physical characteristics of baked carbon mixes employing coal tar and petroleum pitches. J Mat Sci 1978;13:1632–6.
[10] Takabatake M. Development of petroleum pitch derived high performance C/C composite. In: Proceedings of the Eigth Symposium on High-Performance Materials for Severe Environments, Tokyo: R&D Institute of Metals and Composites for Future Industries (RIMCOF), 1997, pp. 273–81.
[11] Williams KPJ, Pitt GD, Batchelder DN, Kip B. Confocal Raman microscopy using a stigmatic spectrograph and CCD detector. Appl Spectrosc 1994;48:232–5.
[12] Tuinstra F, Koenig JL. Raman spectrum of graphite. J Chem Phys 1970;53:1126–30.
[13] Pocsik I, Hundhausen M, Koos M, Ley L. Origin of the D peak in the Raman spectrum of microcrystalline graphite. J Non-Cryst Solids 1998;223:1083–6.
[14] Matthews MJ, Pimenta MA, Dresselhaus G, Dresselhaus MS, Endo M. Origin of dispersive effects of the Raman D band in carbon materials. Phys Rev B 1999;B59:6585.
[15] Lespade P, Marchand A, Couzi M, Cruège F. Caractérisation de matériaux carbones par microscopectrométrie Raman. Carbon 1984;22:375–85.
[16] Cuesta A, Dhamelincourt P, Laureyns J, Martinez-Alonzo A, Tascon JMD. Raman microprobe studies of carbon materials. Carbon 1994;32:1523–32.
[17] Katagiri G, Ishida H, Ishitani A. Raman spectra of graphite edge planes. Carbon 1988;26:565–71.
[18] Siron O, Chollon G, Tsuda H, Yamauchi H, Maeda K, Kosaka K. Microstrutural and mechanical properties of filler-added coal-tar pitch-based C/C composites: the damage and fracture process in correlation with AE waveform parameters. Carbon 2000;38:1369–89.